View metadata, citation and similar papers at core.ac.uk
brought to you by CORE
provided by The University of Utah: J. Willard Marriott Digital Library

Electrical properties of transparent and conducting Ga doped ZnO

V. Bhosle,[a] A. Tiwari,[b] and J. Narayan
Department of Materials Science and Engineering, North Carolina State University, Raleigh, North Carolina 27695-7907

(Received 5 December 2005; accepted 3 May 2006; published online 8 August 2006)

In this paper, we report on the metal-semiconductor transition behavior observed in transparent and conducting ZnO:Ga films grown by pulsed-laser deposition. The electrical resistivity measurements were carried out on ZnO films with varying Ga concentration in the temperature range of 14 to 300 K. The electrical properties were correlated with film structure, and detailed structural characterization was performed using x-ray diffraction, transmission electron microscopy, and x-ray photoelectron spectroscopy. The room-temperature resistivity of these films was found to decrease with Ga concentration up to 5% Ga, and then increase. The lowest value of resistivity (1.4×10^{-4} Ω cm) was found at 5% Ga. Temperature dependent resistivity measurements showed a metal-semiconductor transition, which is rationalized by localization of degenerate electrons. A linear variation of conductivity with $\sqrt{T}$ below the transition temperature suggests that the degenerate electrons are in a weak-localization regime. It was also found that the transition temperature is dependent on the Ga concentration and is related to the increase in disorder induced by dopant addition. The results of this research help to understand the additional effects of dopant addition on transport characteristics of transparent conducting oxides (TCOs) and are critical to further improvement and optimization of TCO properties. © *2006 American Institute of Physics.*
[DOI: 10.1063/1.2218466]

INTRODUCTION

Transparent conducting oxides (TCOs) have found applications in several optoelectronic devices such as light emitting diodes (LEDs), solar cells, and flat panels as well as flexible displays.[1,2] Indium tin oxide (ITO) is the most commonly used TCO for these applications because of its high transmittance in the visible region and a resistivity close to 1.0×10^{-4} Ω cm.[2,3] However, high cost and scarce resources of In limit its usage in these devices. The demand for the above-mentioned applications and devices is increasing continuously and has led researchers to explore alternative materials for the TCO applications. Some of the TCOs which have shown transmittance and resistivity values close to those of ITO are ZnO:Ga, ZnO:Al, Cd_2SnO_4, F:SnO_2, and Nb:TiO_2.[3–8] Among these, ZnO is the most favorable material because of its benign nature and relatively low cost.[4–6] Therefore, there is a considerable interest in understanding the electrical and transport properties of doped ZnO films, which is critical for further improvement of TCO characteristics. It has been suggested that in case of TCOs, electron scattering is mainly caused by ionized impurities, grain boundaries and lattice vibrations.[9–12] Several models have been proposed to predict the limits for the lowest values of resistivity and mobility based on the prominent scattering mechanism.[12–14] However, additional effects on the electrical properties, such as localization, related to the disorder induced by ionized impurities in TCOs have not been addressed adequately. Although there have been a few reports about the observation of weak localization in degenerate TCO films due to disorder, all of these reports are associated with amorphous TCOs.[15,16] In our recent work, we have shown that such phenomena are operative in crystalline TCOs as well.[17] In this paper, we report the observation of a metal-semiconductor transition and discuss the mechanism in terms of localization caused by the disorder induced by Ga dopants in ZnO films. In order to understand the fundamentals of the observed transition, we have investigated the effect of dopant concentration on the temperature dependence of electrical properties. We present optical, structural, chemical, and electrical property measurements to understand interesting characteristics of Ga:ZnO films. The metal-semiconductor transition temperature, which is related to the degree of disorder, is found to be dependent on dopant concentration in TCO films. This study suggests a need to incorporate secondary scattering effects associated with the dopant induced disorder in models used to predict the limits of the physical properties of TCOs.

EXPERIMENTAL DETAILS

Ga doped ZnO films were grown on *c* plane (0001) of sapphire single crystal substrates by a pulsed-laser deposition technique.[18] The ZnO targets doped with different concentrations (2–7 at. %) of gallium were prepared by a conventional solid state reaction technique. A pulsed KrF excimer laser with a wavelength of 248 nm was used for ablation. The energy density of the laser beam was varied from 4 to 7 J/cm^2 with a repetition rate of 10 Hz. The chamber was evacuated to a base pressure of 1×10^{-3} torr, and the deposition was carried out at 2×10^{-2} torr of oxygen pressure. The deposition was performed in the temperature range

[a]Electronic mail: vmbhosle@ncsu.edu
[b]Present address: Department of Materials Science and Engineering, University of Utah.

 © 2006 American Institute of Physics

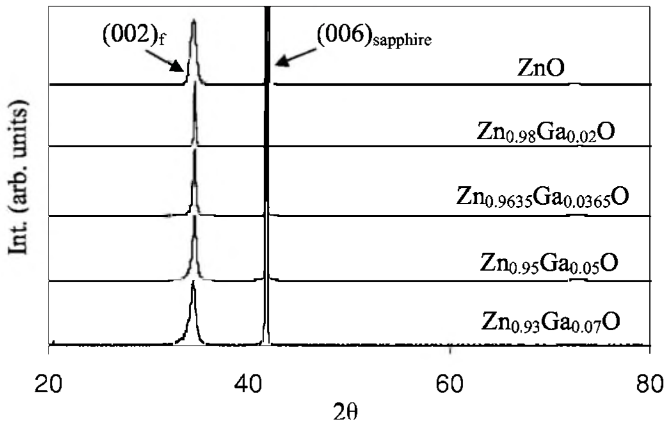

FIG. 1. XRD of ZnO films with different concentrations of Ga deposited at 400 °C and 2×10^{-2} torr of oxygen pressure.

of 400–450 °C for 12 min. Deposition temperature was selected such that the films grew epitaxially with minimal dopant segregation. For a comparison of electrical and optical properties, single crystal epitaxial films with varying concentration of Ga were grown. For x-ray diffraction (XRD), θ-2θ scans of the films were carried out using a Rigaku x-ray diffractometer with Cu $K\alpha$ radiation ($\lambda=1.54$ Å) and a Ni filter. A JEOL-2010 field emission transmission electron microscope (TEM) with a Gatan image filter (GIF) attachment was used to perform detailed structural characterization of the films. Chemical analysis of the films was done using x-ray photoelectron spectroscopy (XPS) with a Riber LAS-3000 instrument with a Mg $K\alpha$ x-ray source. Analysis of the oxidation states from the spectrum was performed by deconvolution using a Shirley routine and a Casa software.[19] The values corresponding to the C 1s peak were used as a reference for the curve fitting analysis. Optical measurements (absorption and transmission) were made using a Hitachi U-3010 spectrophotometer, while the electrical resistivity was measured using the four-point probe technique. The electrical resistivity was measured in the temperature range of 15–300 K as a function of Ga concentration to establish structure-property correlations.

RESULTS AND DISCUSSION

Structural characterization

Figure 1 shows XRD results (θ-2θ scans) of the films with different concentrations of Ga grown at 400 °C and 2×10^{-2} torr. These patterns show that the films are highly textured along the c axis which is designated as the (0006) peak of sapphire. The absence of additional peaks in the XRD pattern excludes the possibility of any extra phases and/or large-size precipitates in the films. Detailed TEM analysis was performed using X-sectioned samples to further analyze microstructure and epitaxial characteristics. Figure 2(a) is a high resolution TEM (HRTEM) image of a $Zn_{0.95}Ga_{0.05}O$ sample, from which it can be seen that the film has grown epitaxially on a (0001) sapphire substrate. The film is free of any nanosized clusters or precipitates, which might have been difficult to detect by XRD. Similar observations were found for ZnO films doped with other

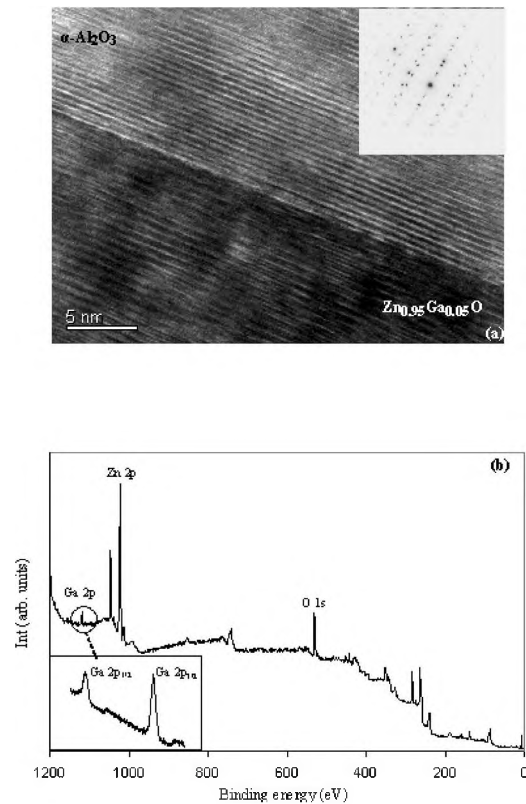

FIG. 2. (a) HRTEM of the interface. The inset shows the SAED pattern. (b) Survey XPS spectrum from the surface of $ZnGa_{0.05}O$ film deposited at 400 °C and 2.4×10^{-2} torr. The inset shows the high resolution spectrum of the Ga 2p peaks.

concentrations of Ga. A selected area electron diffraction (SAED) pattern taken from the interface is shown as an inset in Fig. 2(a), from which we can determine the following epitaxial relationship: $(0002)_f \| (0002)_s$, $(\bar{2}110)_f \| (01\bar{1}0)_s$, and $(01\bar{1}0)_f \| (\bar{2}110)_s$. This epitaxial relationship corresponds to a 30° or 90° rotation in the basal plane of the sapphire (0001) substrate. The epitaxy in such a large (16%) misfit system occurs as a result of domain matching epitaxy, where integral multiples of planes match across the film substrate interface.[20] In the present case six $(01\bar{1}0)_f$ planes of the film match with seven $(\bar{2}110)_s$ planes of the sapphire substrate. Chemical analysis of these films was performed using XPS to determine the extent and nature of Ga solubility in ZnO. From a high resolution XPS spectrum shown in Fig. 2(b), the positions of Ga $2p_{3/2}$ and Ga $2p_{1/2}$ peaks were found to be at 1119.0 and 1146.2 eV, respectively. These peak positions are in good agreement with the previously reported values,[21] which suggests that Ga exists as Ga^{3+}. The absence of any Ga clusters as determined from the HRTEM and XRD analyses indicates that Ga^{3+} occupies Zn substitutional sites and, therefore, can act as an effective donor.

Electrical and optical properties

The effect of doping was studied by measuring the electrical and optical properties of the films with different concentrations of Ga. Figure 3 shows the effect of film compo-

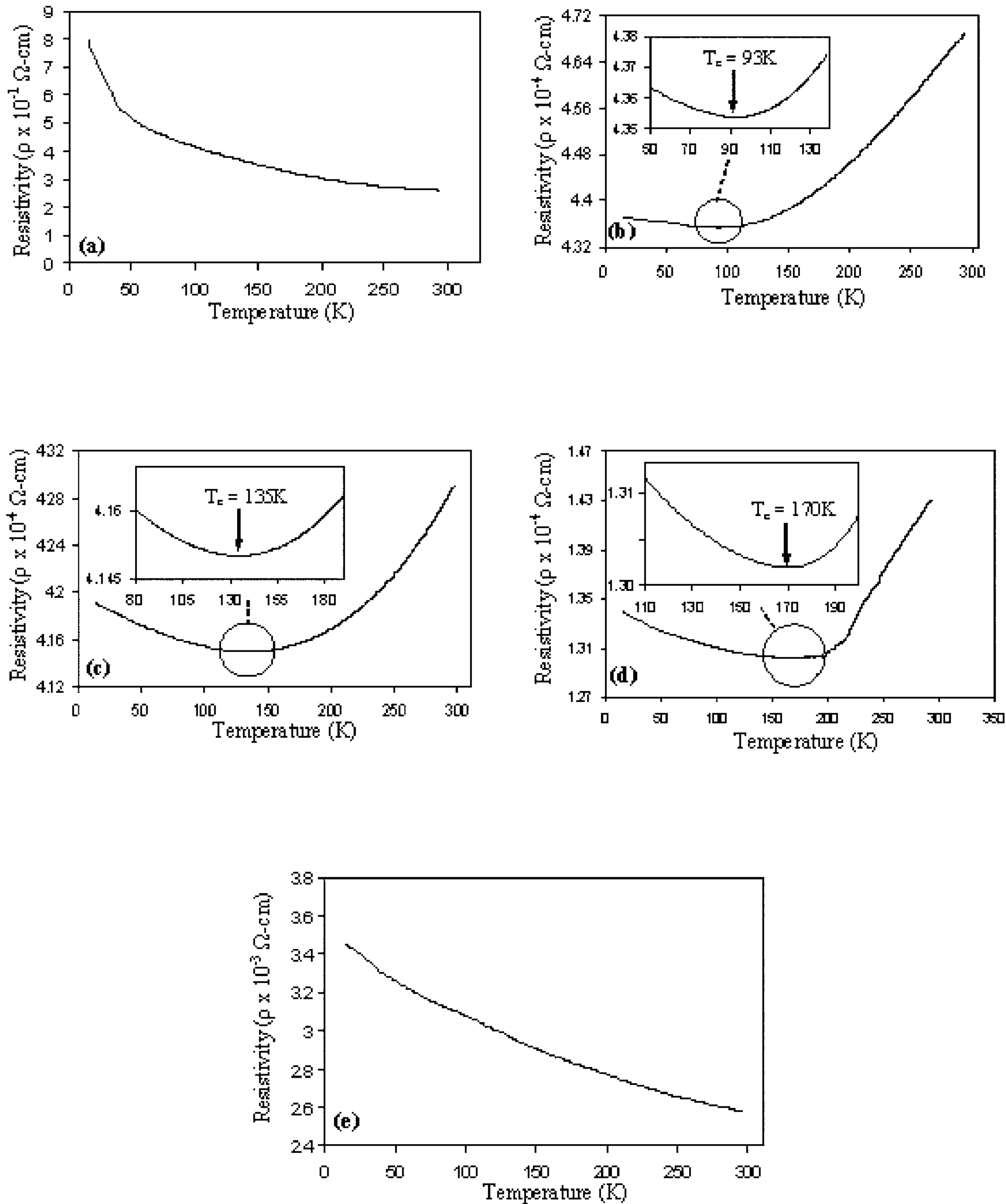

FIG. 3. Plot of resistivity vs temperature for (a) undoped ZnO film, (b) $Zn_{0.98}Ga_{0.02}O$, (c) $Zn_{0.965}Ga_{0.0365}O$, (d) $Zn_{0.95}Ga_{0.05}O$, and (e) $Zn_{0.93}Ga_{0.07}O$.

sition on the temperature dependence of resistivity for Ga doped ZnO films. Figures 3(a)–3(e) correspond to gallium concentrations of 0%, 2%, 3.65%, 5%, and 7%, respectively. Pure ZnO shows relatively high resistivity at room temperature (RT) and a negative temperature coefficient of resistivity (TCR), characteristic of semiconducting behavior. However, with the addition of Ga, the RT values of resistivity decrease by two to three orders of magnitude. It can be seen from Figs. 3(b)–3(e), that the RT resistivity decreases continuously as the Ga concentration is increased up to 5%, beyond which the resistivity was found to increase again. The values of resistivity for different Ga doped ZnO films are listed in Table I. The increase in conductivity can be explained by the increase in carrier concentration due to Ga addition. The in-

TABLE I. List of values of resistivity and the metal-semiconductor transition temperature of ZnO films with varying Ga concentrations.

% Ga	Resistivity (Ω cm)	T_c (measured) (K)	$L_i = d_{Ga}$ (nm)	T_c (calculated) (K)
0	2.59×10^{-1}	...	...	...
2	4.71×10^{-4}	93	1.33	92
3.65	4.29×10^{-4}	135	1.10	134
5	1.40×10^{-4}	170	0.98	171
7	2.57×10^{-3}	...	...	...

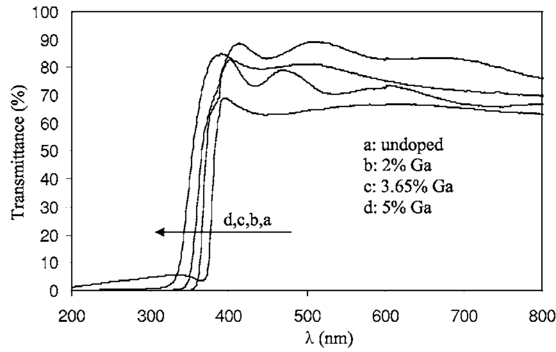

FIG. 4. Transmission spectra of films with different concentrations of Ga.

creased carrier concentration also leads to a metallic behavior at temperatures closer to the ambient temperature, which is not observed in pure ZnO. Metallic conductivity is observed in samples containing 2%, 3.65%, and 5% Ga due to the formation of a degenerate band appearing in heavily doped semiconductors, as suggested by Mott.[22] The increase in carrier concentration is also consistent with the optical results, as shown in Fig. 4. This figure illustrates transmission spectra of ZnO films with different concentrations of Ga. The absorption edge shows a continuous shift towards higher energy with the increase in Ga concentration according to the Burnstein-Moss effect.[23,24] The shifts observed in the transmission spectra are in good agreement with observations reported by other researchers.[5] Photoluminescence measurements also showed similar peak shifts, further strengthening our supposition that the carrier concentration is increased by Ga addition, thus lowering the resistivity of ZnO films. Although Ga increases the carrier concentration and conductivity in ZnO, it also tends to affect the carrier transport, as is evident at lower temperatures. From Figs. 3(b)–3(d) it can be seen that a minimum in resistivity is observed at low temperatures for samples containing 2%, 3.65%, and 5% Ga, respectively. The transition from metallic to semiconductor behavior suggests that more than one competing mechanisms are operative. The negative TCR observed below the transition temperature (T_c) indicates localization of electrons.[25] A detailed analysis was performed to understand the exact nature of the interactions occurring at lower temperatures. If the electrons are localized due to a strong interaction, similar to the Anderson localization, the conduction occurs by thermally activated motion, which is known as the variable range hopping (VRH) mechanism. The conductivity in this case is given by the expression[25,26]

$$\sigma = A \exp(-B/T^{1/4}), \tag{1}$$

where $B=4E/(k_B T^{3/4})$, E is the activation energy, and A is a preexponential constant. The conductivity data corresponding to Figs. 3(b)–3(e) showed a decent fit to the above expression for temperatures below the transition, and the values of activation energy calculated from the slope were found to be on the order of a few meV (2% Ga=0.026 meV, 3.65% Ga=0.05 meV, 5% Ga=0.18 meV, and 7% Ga=0.422 meV). These values are extremely small compared to kT, which suggests that the conduction does not occur by activated motion and electrons seem to be weakly localized. In the weakly localized regime, electrical conductivity is given by the expression[16,25,27]

$$\sigma = \sigma_B \left[1 - \frac{C}{(k_F l)^2} \left(1 - \frac{l}{L_i} \right) \right], \tag{2}$$

where σ_B is the Boltzmann's conductivity, C is a constant of the order 1, l is the mean free path, and L_i is the inelastic diffusion length equal to $\sqrt{D\tau_i}$. Also, since $\tau_i \alpha 1/T$, $L_i = (\hbar D/k_B T)^{1/2}$, which leads to $\sigma \alpha T^{1/2}$. In a system with disorder, localization occurs due to the constructive interference of scattered electrons, which decreases the conductivity.

In Eq. (2), the term $[C/(k_F l)^2](1-l/L_i)$ represents the reduction in localization caused by the constructive interference of scattered electrons. The term inside the bracket signifies that L_i decreases with an increase in temperature due to increased inelastic scattering and tends to increase the conductivity, thus leading to the negative TCR. Figure 5(a) is a plot of conductivity versus $\sqrt{T}$ for the sample containing 5% Ga. The constant slope suggests that the conductivity is governed by weak localization at lower temperatures. A similar behavior can be seen in Figs. 5(b), 3(c), and 3(d) corresponding to the $Zn_{0.98}Ga_{0.02}O$, $Zn_{0.9635}Ga_{0.0365}O$, and $Zn_{0.93}Ga_{0.07}O$ compositions, respectively. At higher temperatures, Ga doped ZnO is degenerate and shows a metallic behavior where the conductivity is dominated by phonon scattering. However, as the temperature decreases, L_i increases, and when L_i is equal to the distance between the Ga atoms (d_{Ga}), electrons start to interfere constructively. This leads to localization of electrons, and the term represented inside the bracket in Eq. (2) tends to dominate the conductivity. Thus, at temperatures above T_c, electrons can be considered to be completely delocalized, leading to metallic conductivity, which is characteristic of a degenerate semiconductor. Also, it can be observed from Figs. 3(b)–3(d) that as the dopant concentration increased, the transition temperature increased and electron localization shifted toward higher temperatures. This can be explained by considering the increase in disorder caused by the dopant addition. As the amount of Ga increases, the distance between the dopant atoms decreases, leading to an increase in disorder and causing the electrons to interfere at shorter values of L_i, thus increasing the temperature at which localization occurs. To verify this we calculated the transition temperature using the relation $L_i = (\hbar D/k_B T)^{1/2}$, where L_i was taken to be equal to the distance between the dopant atoms for a given concentration ($d_{Ga} = N_{Ga}{}^{1/3}$). The temperatures calculated using the above formula were found to be in close agreement with the experimentally observed values of T_c, which further substantiates our explanation. All the values calculated for different concentrations of Ga have been tabulated in Table I. For a sample with 7% Ga, no transition is observed, and it shows only a negative TCR in the temperature range of 14–300 K. In addition, it also shows a considerably higher value of resistivity at RT, as compared to other Ga doped ZnO films. Although the data still obeys the temperature dependence given by Eq. (2), the increased RT value of resistivity indicates that the system is driven towards the strong-

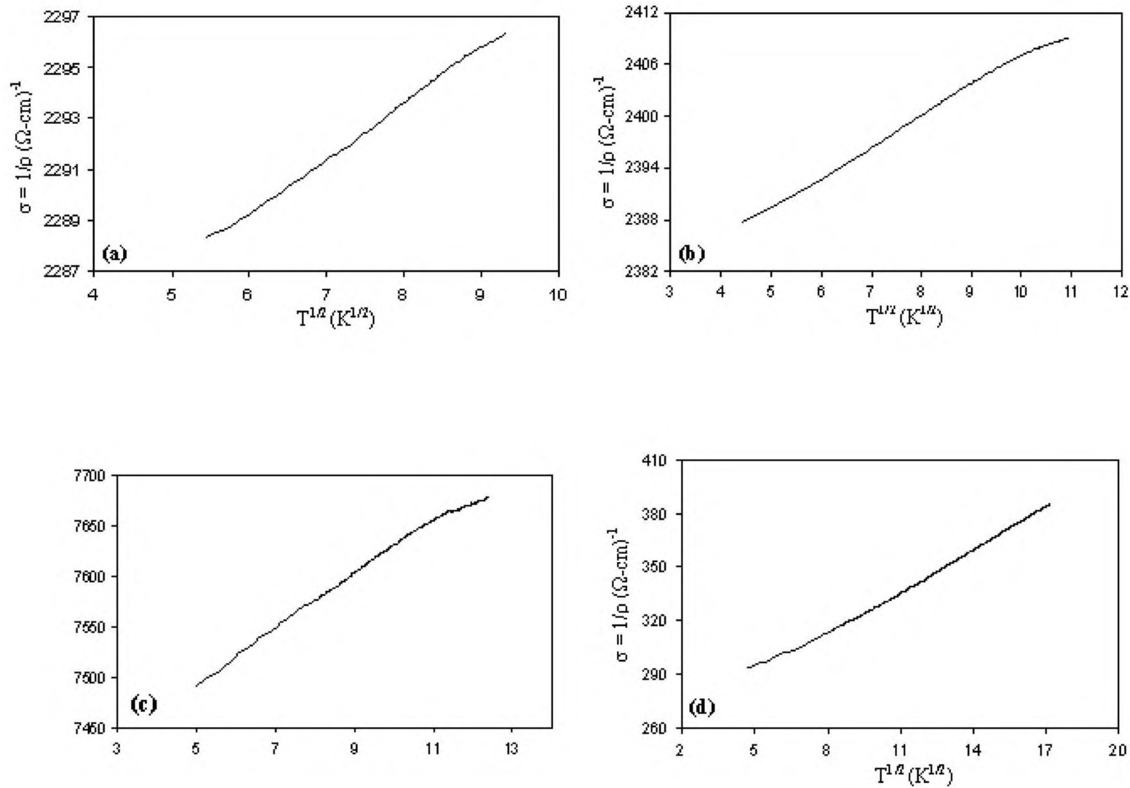

FIG. 5. Plot of σ vs $\sqrt{T}$ at temperatures below the transition for (a) $Zn_{0.98}Ga_{0.02}O$, (b) $Zn_{0.965}Ga_{0.0365}O$, (c) $Zn_{0.95}Ga_{0.05}O$, and (d) $Zn_{0.93}Ga_{0.07}O$.

localization regime as the disorder due to Ga atoms is increased beyond a critical limit, which in this case is found to be close to 5%.

CONCLUSION

In summary, we have grown epitaxial ZnO films doped with Ga on single crystal (0001) sapphire substrates and investigated the effect of Ga addition on transport properties of these films. Room-temperature resistivities of the films were found to decrease with an increase in Ga concentration up to 5% Ga, which showed the lowest value of resistivity. Detailed cross-sectional TEM studies confirmed the epitaxial nature of the films and also suggested the absence of extra phases and/or nanoclusters. XPS analysis revealed that Ga is present as Ga^{3+} and, therefore, can act as an effective donor. The epitaxial nature of the films minimizes the scattering due to defects and facilitates the identification of conduction mechanisms. The temperature dependent resistivity of these films showed a metal-semiconductor transition, which indicates that secondary scattering effects such as localization due to disorder induced by dopant addition are important in crystalline TCOs. A linear variation of conductivity with $\sqrt{T}$ below the transition temperature suggests that the degenerate electrons are in a weak-localization regime. The metal-semiconductor transition temperature was found to be dependent on the dopant concentration in the ZnO and was related to the increase in disorder induced by Ga atoms. When the concentration of Ga was increased beyond 5%, the films show only negative TCR and an increase in RT resistivity, which indicates that the system is driven further towards the strong-localization regime. Thus, we have shown that highly conducting and transparent ZnO:Ga films can be grown on sapphire at 400 °C and the conductivity can be controlled by the dopant concentration. Additional effects of dopants on transport characteristics were also found from our temperature dependent study of electrical properties, resulting in a better understanding of the conduction mechanisms in TCOs. Such studies are likely to aid further optimization of the properties of TCOs and to highlight the need to incorporate secondary scattering effects associated with dopant induced disorder in the models used to predict the limits of the physical properties of TCOs.

ACKNOWLEDGMENT

This research was supported by the National Science Foundation.

[1] D. S. Ginley and C. Bright, MRS Bull. **25**, 15 (2000).
[2] T. Minami, MRS Bull. **25**, 38 (2000).
[3] T. Minami, Semicond. Sci. Technol. **20**, S35 (2005).
[4] A. Suzuki, T. Matsushita, T. Aoki, Y. Yoneyama, and M. Okuda, Jpn. J. Appl. Phys., Part 2 **38**, L71 (1999).
[5] B. H. Choi, H. B. IM, J. S. Song, and K. H. Yoon, Thin Solid Films **193**, 712 (1990).
[6] H. Hirasawa, M. Yoshida, S. Nakamura, Y. Suzuki, S. Okada, and K. Kondo, Sol. Energy Mater. Sol. Cells **67**, 231 (2001).
[7] R. G. Gordon, MRS Bull. **52**, 15 (2000).
[8] Y. Furubayashi, T. Hitosugi, Y. Yamamoto, K. Inaba, G. Kinodo, Y. Hirose, T. Shimada, and T. Hasegawa, Appl. Phys. Lett. **86**, 252101 (2005).
[9] D. H. Zhang and H. L. Ma, Appl. Phys. A: Mater. Sci. Process. **62**, 487 (1996).

[10]H. Brooks, Adv. Electron. Electron Phys. **7**, 85 (1955).
[11]R. B. Dingle, Philos. Mag. **46**, 831 (1955).
[12]I. Hamberg and C. G. Granqvist, J. Appl. Phys. **60**, R123 (1986).
[13]J. R. Bellingham, W. A. Phillips, and C. J. Adkins, J. Mater. Sci. Lett. **11**, 263 (1992).
[14]M. Chen, Z. L. Pei, X. Wang, Y. H. Hu, X. U. Liu, C. Sun, and L. S. Wen, J. Phys. D **33**, 2538 (2000).
[15]C. J. Adkins, T. Hussain, and N. Ahmad, J. Phys.: Condens. Matter **5**, 6647 (1993).
[16]K. Shimakawa, S. Narushima, H. Hosno, and H. Kawazoe, Philos. Mag. Lett. **79**, 755 (1999).
[17]V. Bhosle, A. Tiwari, and J. Narayan, Appl. Phys. Lett. **88**, 032106 (2006).
[18]D. B. Chrisey and G. H. Hubler, *Pulsed Laser Deposition of Thin Films* (Wiley, New York, 1994).
[19]N. Fairley and A. Carrick, *The Casa Cookbook: Recipes for XPS Data Processing* (Acolyte Science, Cheshire, 2005), Pt. 1 (http://www.casaxps.com/).
[20]J. Narayan and B. C. Larson, J. Appl. Phys. **93**, 278 (2003).
[21]M. Passlack *et al.*, J. Appl. Phys. **77**, 686 (1995).
[22]N. F. Mott, *Metal-Insulator Transition* (Taylor & Francis, London, 1974).
[23]E. Burstein, Phys. Rev. **93**, 632 (1954).
[24]T. S. Moss, Proc. Phys. Soc. London, Sect. B **67**, 775 (1954).
[25]N. F. Mott, *Conduction in Non-Crystalline Materials* (Claderon, Oxford, 1993).
[26]C. Ang, J. R. Jurado, Z. Yu, M. T. Colomer, J. R. Frade, and J. L. Baptista, Phys. Rev. B **57**, 11858 (1998).
[27]M. Kaveh and N. F. Mott, Philos. Mag. B **50**, 175 (1983).